Robby WEIMER

Biologie Cellulaire de la Synapse N&P
I.N.S.E.R.M. U. 497
ECOLE NORMALE SUPÉRIEURE
46, rue d'Ulm 75005 PARIS
Tél: 33 (0) 1 44 32 23 09
Fax: 33 (0) 1 44 32 36 54
email: weimer@biologie.ens.fr

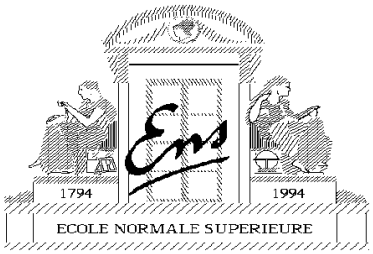

Dear Reader,

There is an error on the accompanying manuscript. In the Material and Methods section under the heading of Chemical Fixation and Freeze-substitution (page 2) the concentration of osmium listed is 0.01% when, in fact, the concentration used was 1% in acetone.

Volume 52(1): 1–12, 2004
Journal of Histochemistry & Cytochemistry
http://www.jhc.org

RAPID COMMUNICATION

Preservation of Immunoreactivity and Fine Structure of Adult *C. elegans* Tissues Using High-pressure Freezing

Philippe Rostaing,[1] Robby M. Weimer,[1] Erik M. Jorgensen, Antoine Triller, and Jean-Louis Bessereau

Biologie Cellulaire de la Synapse, École Normale Supérieure, Paris, France (PR,RMW,AT,J-LB); and Department of Biology, University of Utah, Salt Lake City, Utah (EMJ)

SUMMARY The location of a protein labeled by immunogold techniques can be resolved under an electron beam to within nanometers of its epitope, a resolution that makes immunoelectron microscopy a valuable tool for studies of cell biology. However, tissues in the nematode *Caenorhabditis elegans* are difficult to preserve for immunoelectron microscopic studies. The animal's cuticle slows the diffusion of solutions into the animal and thus makes it difficult to preserve both immunoreactivity and cell morphology. Here we describe a protocol that circumvents these problems. Specifically, we instantly immobilized tissue in vitreous ice by freezing living adult animals under high pressure. Frozen specimens were then chemically fixed, dehydrated, and embedded at low temperatures. As a result, chemical diffusion across the cuticle could occur over an extended period without morphological deterioration. We show that this method is capable of preserving both cell morphology, including fine structures, and immunoreactivity. Therefore, it provides a means to characterize the localization of endogenous proteins and exogenous proteins, such as the green fluorescent protein (GFP), with respect to subcellular compartments in *C. elegans* tissues by using postembedding immunogold labeling. **(J Histochem Cytochem 52:1–12, 2004)**

KEY WORDS
C. elegans
immunoelectron microscopy
high-pressure freezing
immunogold

The soil nematode *Caenorhabditis elegans* is an excellent model system for cell biology studies. In *C. elegans*, genetic tools can be employed to identify and inactivate proteins of interest (Brenner 1974; Zwaal et al. 1993; Jansen et al. 1997; Fire et al. 1998), molecular techniques can be used to express engineered forms of proteins in vivo (Fire and Waterston 1989; Mello et al. 1991), and the functional consequence of protein alteration can be studied in the context of an entire animal. In addition, protein distribution can be studied with relative ease by light microscopy. For example, proteins tagged with the green fluorescent protein (GFP) can be visualized in a living animal under a fluorescence microscope (Chalfie et al. 1994). However, the resolution of light microscopy is inadequate to characterize a protein's distribution relative to subcellular structures. For such studies the electron microscope is necessary because a protein labeled by immunogold staining can be visualized at a resolution of a few nanometers (Faulk and Taylor 1971). However, protein localization studies in the nematode at the level of the electron microscope have been limited, primarily due to the difficulty of passing solutions across the low-permeability cuticle that encases the animal.

For classical electron microscopy studies in *C. elegans*, such as those conducted to describe its anatomy (Epstein et al. 1974; Waterston et al. 1974; Ward et al. 1975; Albertson and Thomson 1976; White et al. 1976,1986), best preservation and embedding is obtained from animals that have been cut to allow chemical fixatives and embedding solutions access to inner tissues. In combination with strong fixative reagents, such as osmium tetroxide, excellent preservation for ultrastructural studies is achieved; however, immunoreactivity is lost. If weaker fixative reagents are used, such as paraformaldehyde, proteins often remain antigenic (Park et al. 2001) but structural preservation is compromised. Recent attempts to remedy this para-

Correspondence to: Jean-Louis Bessereau, Biologie Cellulaire de la Synapse, École Normale Supérieure, 46 rue d'Ulm, Paris 75005 France. E-mail: jlbesse@wotan.ens.fr

Received for publication June 30, 2003; accepted August 27, 2003 (3C6122).

[1]These authors contributed equally to this work.

0022-1554/04/$3.30

dox in *C. elegans* immunoelectron microscopy have taken two approaches: increase cuticle permeability or physically immobilize tissues before chemical fixation.

To increase cuticle permeability, Paupard et al. (2001) exposed intact animals to microwaves. The rate of diffusion after exposure to microwaves was sufficient to preserve gross cell structure and protein immunoreactivity. However, fine structures, such as those in neurons, were not well preserved (Paupard et al. 2001).

To physically immobilize tissues before chemical fixation, Kirkham et al. (2003) froze *C. elegans* embryos under high pressure and then chemically fixed the specimens at low temperatures, a strategy recently used for morphological studies in *C. elegans* (Dernburg et al. 1998; Williams–Masson et al. 1998; Rappleye et al. 1999; Howe et al. 2001; Koppen et al. 2001; MacQueen et al. 2002; Rolls et al. 2002) and for immunoelectron microscopy studies in other organisms (reviewed in McDonald 1999). Freezing under high pressure is capable of solidifying water rapidly as vitreous ice, an amorphous state of water, which physically preserves tissues. Chemical tissue fixation and embedding can then occur over an extended period of time without deterioration of the tissue ultrastructure. In the embryo, overall cell structure as well as protein immunoreactivity were well preserved after high-pressure freezing. In addition, high-pressure freezing has been used to detect cuticle antigens in dauer arrested larvae (Favre et al. 1995,1998). These results suggested that a similar method might be suitable for studies in the adult.

Here we describe a protocol for the preservation of adult tissues in *C. elegans* for immunoelectron microscopy studies. Specifically, living animals are immobilized by high-pressure freezing, then chemically fixed, dehydrated, and embedded at low temperatures over an extended period of time. With this protocol, cell morphology is well preserved, including fine structures such as microtubules and actin–myosin lattices. In addition, protein immunoreactivity is preserved. We successfully stained ultrathin sections with antibodies directed against components of fibrous organelles, cell adhesion junctions, and synaptic vesicles, and an exogenous GFP fusion protein expressed in neurons. This protocol therefore provides a method for localization of endogenous and exogenous proteins with respect to subcellular compartments in most, if not all, *C. elegans* tissues.

Materials and Methods

Classical Electron Microscopy

Young adult hermaphrodites, cultured under standard conditions (Brenner 1974), were prepared by classical fixation for transmission electron microscopy as described previously (Jorgensen et al. 1995). Specimens were fixed in 0.7% glutaraldehyde, 0.7% osmium tetroxide in 10 mM HEPES buffer for 1 hr, then washed in 10 mM HEPES buffer. Next, the animals' heads and tails were removed and the tissue was postfixed in 2% osmium tetroxide in 10 mM HEPES buffer for 3 hr and then washed extensively in water. Specimens were then stained en bloc in 1% uranyl acetate, dehydrated with ethanol, passed through propylene oxide, and embedded in epoxy resin. Ribbons of ultrathin sections (35 nm) were collected for imaging without counterstaining.

High-pressure Freeze Immobilization

N2 Bristol or EG1399[*lin-15(n765)X; oxEx81(Pacr-5::GAP-43-GFP, lin-15*(+))] (Knobel et al. 2001) worms were cultured under standard conditions (Brenner 1974) at 20C and young adult hermaphrodites were immobilized in *E. coli* by high-pressure freezing. Specifically, ~10 animals were placed in a specimen chamber of 100-μm depth (Bal-Tec, Liechtenstein; part number LZ02135VN A and B) filled with *E. coli* (OP50) and frozen rapidly at −176C under high pressure (P >2100 bar) in a Bal-Tec HPM010 apparatus according to the manufacturer's recommendation. Chambers containing frozen specimens were stored in liquid nitrogen.

Chemical Fixation and Freeze-substitution

Frozen animals were chemically fixed and dehydrated in a Reichart AFS apparatus (Leica; Oberkochen, Germany). Specimen chambers were moved into either anhydrous acetone (Carlo Erba; Rodano, Italy) containing 0.01% osmium tetroxide (Polyscience) or anhydrous methanol (Carlo Erba) containing 4% paraformaldehyde (Riedel-de Haën; Seelze, Germany) and 1.5% uranyl acetate (Sigma; St Louis, MO) at −90C. Once placed in the cold fixative solution, the specimen chamber lids were removed. Samples were incubated for 7 days with one change of solution midway through incubation. Frozen EG1399 animals were incubated with anhydrous methanol containing 1.5% uranyl acetate without paraformaldehyde.

Embedding

Animals fixed in osmium were washed in anhydrous acetone then embedded in Araldite (Ernest F. Fullam; Latham, NY) and those fixed in paraformaldehyde were washed in anhydrous methanol, then embedded in Lowicryl HM20 (Polysciences; Warrington, PA) in the following manner. First, the temperature in the Reichart AFS was progressively raised to −45C in increments of 4C/hr. Specimen chambers were placed in wash solution and the frozen galette of worm and bacteria was removed by either suction from a pipette or scraping with a needle. Galettes were further washed with 10-min incubations until the solution remained clear (at least three times) before infiltration. For embedding in Araldite, the galettes were slowly warmed to 20C by incubation at −20C overnight, −4C for 1 hr, and room temperature (RT) for 1 hr, then placed in a Beem capsule cap and infiltrated with resin by incubation in 50% Araldite in acetone for 3 hr at 20C, 90% Araldite in acetone overnight at 4C, and twice in pure Araldite at 20C before polymerization at 60C over 48 hr. After osmium fixation, animals appear light brown within the resin block. For embedding in Lowicryl, the galettes were kept at −45C in the Reichart AFS while be-

ing moved to a Beem capsule cap and placed in a 1:2 solution of Lowicryl to methanol for 12 hr, then in 2:1 Lowicryl to methanol for 12 hr, then pure Lowicryl for 3 days with one change of Lowicryl. Lowicryl was polymerized by UV exposure for 60 hr. After polymerization the temperature of the embedded galette was raised to RT at a rate of 6.5C/hr. After paraformaldehyde fixation animals appear opaque.

Mounting Galettes for Sectioning

Once polymerized, the galettes were examined under a dissecting microscope to identify an appropriate sectioning path, split by cutting with a razor blade to isolate worms to be sectioned, and glued to an Araldite block with Superglue for sectioning. Typically, several worms can be mounted from an individual galette on independent blocks and sectioned in a desired orientation.

Antibodies

The mouse monoclonal antibodies MH27 (Francis and Waterston 1991; an anti-AJM-1 antibody (Koppen et al. 2001) and anti-UNC-17 (Lickteig et al. 2001) were diluted 1:200 and 1:10, respectively. Rabbit polyclonal antisera AF2 (an anti-VAB-10A antibody; Bosher et al. 2003) and Molecular Probes (Eugene, OR) a11122 (an anti-GFP antibody) were diluted 1:2000 and 1:200, respectively.

Immunogold Labeling

Thin (~40- or ~80-nm) sections of Lowricryl-embedded worms were collected on formvar-coated nickel slot grids (Pelanne Instruments; Toulouse, France). For staining with MH27, AF2 and a11122 antibodies, sections on slot grids were blocked in a 5% BSA Cohn Fraction V (Research Organics; Cleveland, OH) PBST (PBS, pH 7.4, with 0.01% Tween-20; Merck, Whitehouse Station, NJ) solution for 30 min at RT then washed three times in 0.1% BSA–PBST for 5 min each. Grids were then incubated in a humidified chamber with dilute primary antibody, described above, in 0.01% CWFS gelatin (Aurion; Wageningen, Netherlands) 0.001% Tween-20–PBS for 1 hr at RT, washed six times in 0.1% BSA–PBST, incubated in a humidified chamber with goat anti-rabbit or anti-mouse 10- or 15-nm gold-conjugated antibodies (BBInternational; Cardiff, UK) diluted 1:200 in 0.01% gelatin–0.001% Tween-20–PBS. After exposure to secondary antibody for 30 min, grids were washed six times in 0.1% BSA–PBST, three times in PBS, fixed in 2% glutaraldehyde (TAAB; Poole, UK) PBS then washed once in PBS and twice in dH_2O.

For staining with the anti-UNC-17 antibody, sections on slot grids were blocked in a 1% goat serum (Aurion) for 30 min at RT, then washed three times in PBS for 5 min each. Grids were then incubated in a humidified chamber with dilute primary antibody in 0.5% CWFS gelatin (Aurion)–0.001% Tween-20–PBS for 1 hr at RT, washed six times in PBS, incubated in a humidified chamber with goat anti-mouse 10-nm gold conjugated antibodies (BBInternational) diluted 1:50 in 0.5% gelatin–0.001% Tween-20–PBS. After exposure to secondary antibody for 30 min, grids were washed nine times in PBS, fixed in 2% glutaraldehyde–PBS, then washed once in PBS and twice in dH_2O. Unless otherwise stated, the specificity of staining was judged by the signal-to-noise ratio for each primary antibody, which was calculated by dividing the bead density in specified tissues by the density within neighboring *E. coli* on the section.

Counterstaining

Before examination, some sections were counterstained by incubating with 2.5% uranyl acetate in 70% methanol for 4 min, followed by washing and incubating with lead citrate (0.15 M lead nitrate, 0.12 M sodium citrate in CO_2-free dH_2O) for 2 min.

Results

Osmium Fixation

The preservation of adult *C. elegans* tissues after immobilization by high-pressure freezing and fixation with osmium tetroxide was recently reported (Dernburg et al. 1998; Williams–Masson et al. 1998; Rappleye et al. 1999; Howe et al. 2001; Koppen et al. 2001; MacQueen et al. 2002; Rolls et al. 2002). Micrographs depicted the excellent preservation of subcellular structures. Specifically, Rolls et al. (2002) report that membrane organelles, such as the endoplasmic reticulum and mitochondria, are well preserved in seam cells, intestinal cells, and neurons. Because tissue preservation is a key step for further analysis of subcellular protein distribution, we first compared the level of structural preservation achievable in our working conditions to those reported previously and extended the observations to other cell types and structures.

We observed a similar level of preservation throughout the animal after high-pressure freezing (Figure 1). Specifically, in the seam cells membranous structures are well preserved, such as the mitochondrial and endoplasmic reticulum, along with the neighboring excretory canal (Figure 1A). In the intestine, mitochondria, endoplasmic reticulum, and plasma membranes are well preserved (Figures 1B and 1E). Likewise, muscle and epidermal morphology is well preserved (Figures 1C and 1F). The organization of the contractile apparatus remains intact, including the alignment of the dense bodies, M-line, and fibrous organelles. In addition, fine structure within neurons, such as microtubules and synaptic vesicles, is well preserved (Figures 1D and 1G).

During our initial assessment of tissue preservation after high-pressure freeze immobilization, it became apparent that the morphology of tissues differed from that reported previously using classical *C. elegans* fixation, which is performed after the cuticle is cut. These differences are exemplified by comparing the structure of the ventral nerve cord (Figure 2). After classical fixation, neuron processes appear slightly compressed, compacted against other processes, and contain few visible microtubules (Figure 2A). After high-pressure freeze immobilization and chemical fixation, neuron

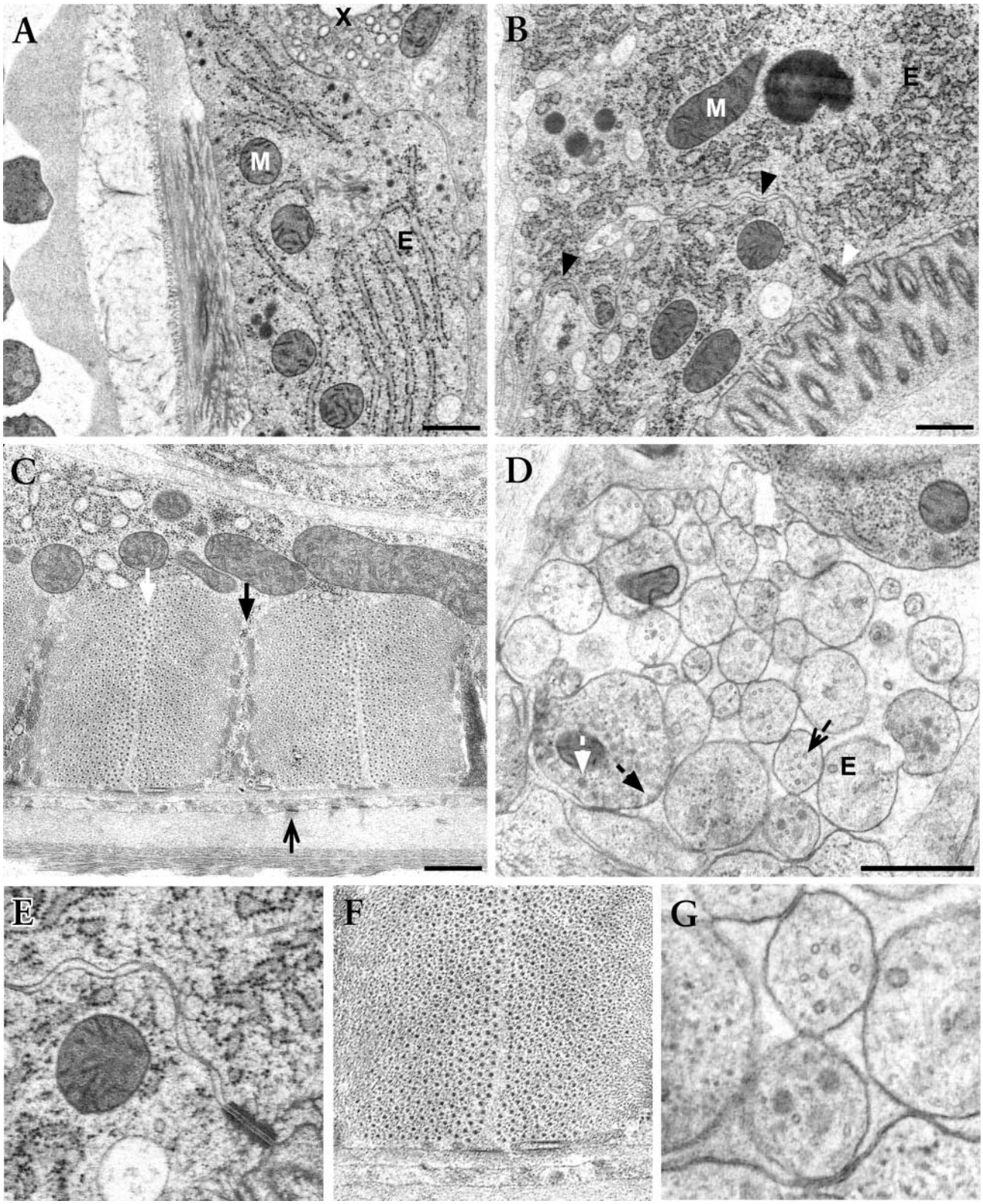

Figure 1 Morphology of tissues after osmium fixation and embedding in Araldite. (**A**) At the animal's periphery, membranous structures are well preserved, such as endoplasmic reticulum (E) and mitochondria (M) in seam cells and the excretory canal (X). (**B**) In internal tissues, such as the intestine, endoplasmic reticulum (E) and mitochondria (M) are well preserved, as well as the plasma membrane (black arrowhead) and cell adhesion sites (white arrowhead). (**C**) Muscle and epidermal cells remain organized such that the dense bodies (black arrow), M-line (white arrow), and fibrous organelles (open arrow) are clearly visible. (**D**) Neurons appear round in the nerve cords—the ventral nerve cord is pictured here—and contain fine structures such as synaptic vesicles (black dashed arrow), dense-core vesicles (white dashed arrow), endoplasmic reticulum (E) and microtubules (open dashed arrow). Bars: **A–D** = 500 nm; **E–G**, twofold enlargement of micrographs in **B–D**, respectively.

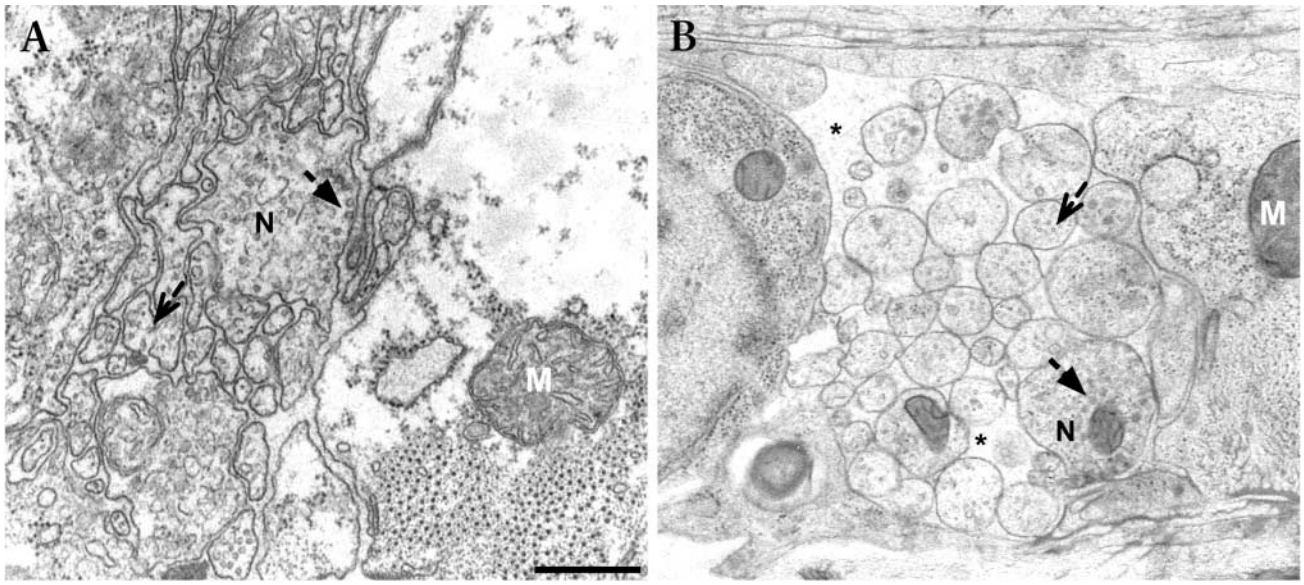

Figure 2 Morphology of classical fixation of *C. elegans* tissues vs high-pressure freezing. (**A**) With classical fixation techniques, cells were exposed to both mechanical and chemical stress before fixation, often resulting in alterations in morphology. For example, neuronal processes (N) within the nerve cord often appear compressed and compacted against neighboring neurons. Synaptic vesicles are clearly visible (black dashed arrow), yet microtubules are rarely observed (open dashed arrow). (**B**) With high-pressure freezing followed by chemical fixation, neuron processes (N) appear round, with space between processes (*), and both synaptic vesicles (black dashed arrow) and microtubules (open dashed arrow) are clearly visible within processes. M, muscle mitochondria. Bar = 500 nm.

processes appear round, with space between neurons, and contain many microtubules (Figure 2B). The differences observed in the structure of the nerve cord could be due to a general swelling artifact caused by the freezing step. However, it is unlikely that swelling occurs, given the speed of the freezing process, which takes place within milliseconds. In addition, several other structures appear similar between the two fixation protocols. In both cases synaptic vesicles are easily identifiable and do not differ in size between fixation protocols (for classical fixation, the average synaptic vesicle diameter is 30.8 ± 1.2 nm, n=4 synaptic vesicles; for high-pressure freeze, the average synaptic vesicle diameter is 31.6 ± 0.2 nm, n=4 synaptic vesicles; p=0.25). The average thickness of the epidermis directly underneath the muscle M-line does not differ between the two protocols (for classical fixation, average thickness is 82.5 ± 4.8 nm, n=4 M-lines; for high-pressure freeze, average thickness is 87.5 ± 4.8 nm, n=4 M-lines; p=0.3). In addition, the average circumference of mitochondria, a difficult structure to preserve, does not differ between the two protocols. For classical fixation, the average circumference of mitochondria cross-sections in muscle is 1580 ± 22.5 nm, n=26 mitochondrial profiles; for high-pressure freezing, the average circumference of mitochondria in muscle is 1463 ± 54.1 nm, n=49 mitochondrial profiles; p=0.05. Therefore, the difference in gross morphology is not likely to be due to a general swelling of tissues after freezing but rather to better preservation of cell morphology and extracellular space by fixation after high-pressure freezing.

Paraformaldehyde Fixation

Both osmium tetroxide and Araldite, the chemical fixative and resin used for the studies discussed above, are incompatible with most immunolabeling protocols. In an attempt to preserve cell morphology along with immunoreactivity, we substituted paraformaldehyde for osmium tetroxide and Lowicryl for Araldite to fix and embed animals after high-pressure freeze immobilization. Cell morphology is well preserved under these conditions (Figure 3). Specifically, in the seam cells the mitochondrial and endoplasmic reticulum membranes are intact, along with the many membranes of the excretory canal (Figure 3A). It is noteworthy that the membranes in these sections have not been stained with osmium and correspondingly appear in lower contrast. In the intestine, the endoplasmic reticulum, mitochondria, and plasma membranes are preserved (Figures 3B and 3E). Dense bodies in the muscle and fibrous organelles in the epidermis are clearly visible (Figures 3C and 3F). The average thickness of the epidermis underneath the muscle M-line is 77.5 ± 7.5 nm, n=4, and the average circumference of mitochondria is 1420 ± 27.7 nm, n=25 mitochondrial profiles. In addition, neuron processes are well preserved, including fine structures such as microtu-

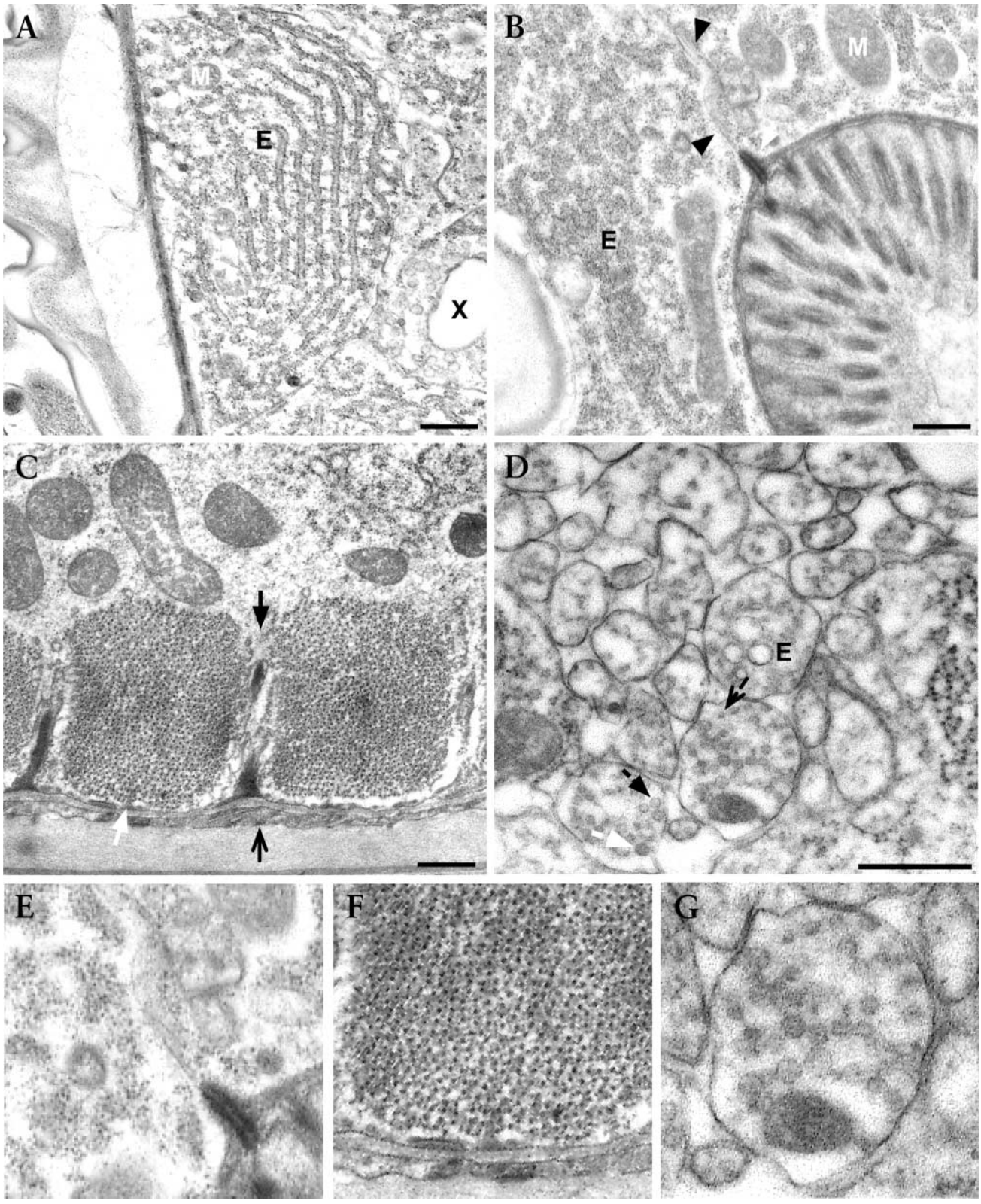

Figure 3 Morphology of tissues after fixation with paraformaldehyde and embedding in Lowicryl HM20. (**A**) Similar to fixation with osmium, fixation with paraformaldehyde is sufficient to preserve membranous structures, such as the endoplasmic reticulum (E) and mitochondria (M) in seam cells, and the excretory canal (X). (**B**) In the intestine, the endoplasmic reticulum (E), mitochondria (M), plasma membrane (black arrowhead), and cell adhesion sites (white arrowhead) are well preserved. (**C**) Muscle and epidermal cells retain much of their organization. Dense bodies (black arrow), M-line (white arrow), and fibrous organelles (open arrow) are clearly visible. (**D**) Neuron structure can also be preserved with paraformaldehyde. Neuron processes in the ventral nerve cord appear round and contain fine structures such as synaptic vesicles (black dashed arrow), dense-core vesicles (white dashed arrow), endoplasmic reticulum (E), and microtubules (open dashed arrow). Bars: **A–D** = 500 nm; **E–G**, twofold enlargement of micrographs in **B–D**, respectively.

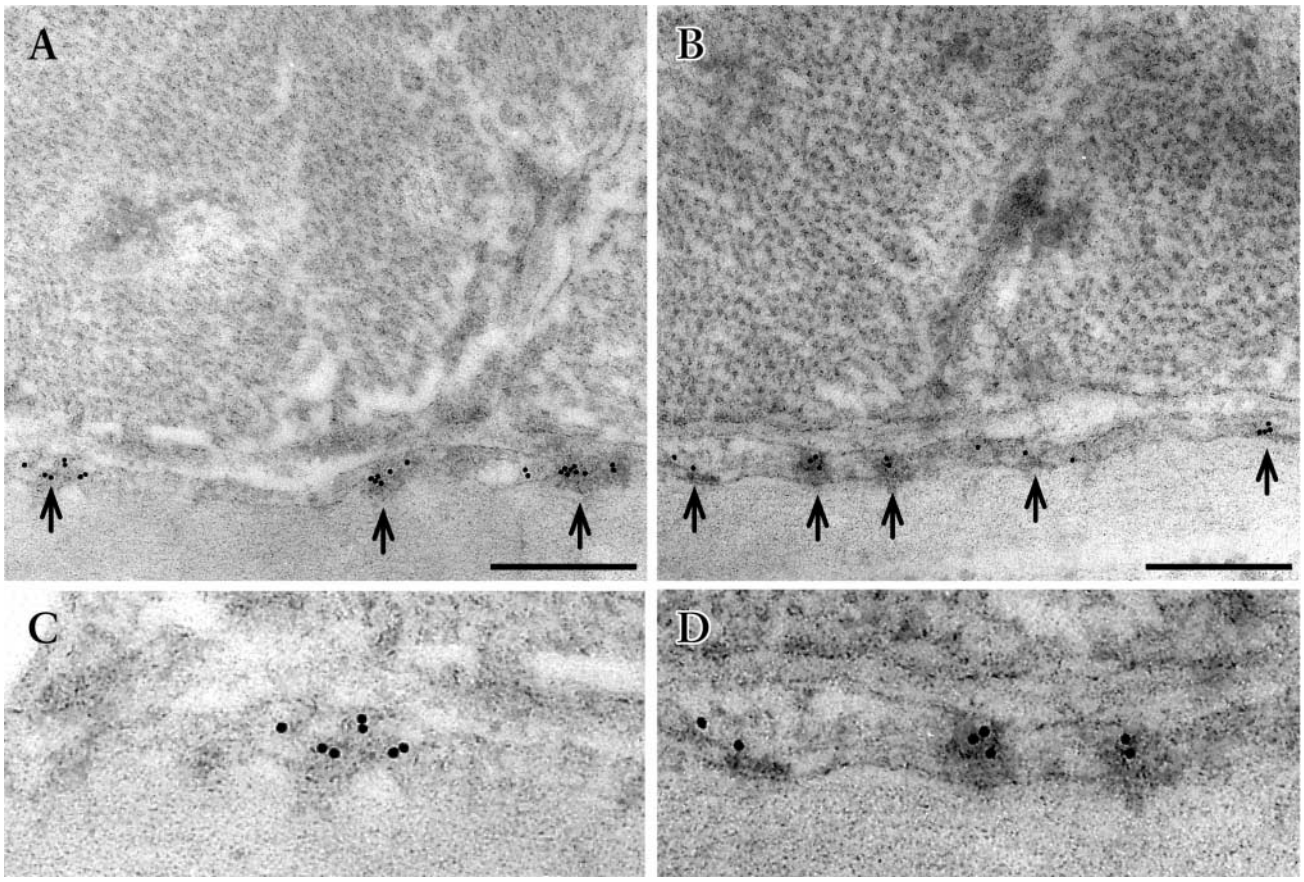

Figure 4 The epidermal protein VAB-10A remains antigenic after high-pressure freezing. Polyclonal antibodies directed against the *C. elegans* plectin homologue VAB-10A localize gold particles to fibrous organelles (open arrow) that attach muscle to the cuticle. **(A,B)** Micrographs from two independent staining experiments. Bars = 500 nm; **(C,D)** Twofold enlargements of **A** and **B**, respectively.

bules and synaptic vesicles (Figures 3D and 3G). The average diameter of a synaptic vesicle is 31.1 ± 1.2 nm, n=4 synaptic vesicles. On the basis of these observations, we conclude that cell morphology, including fine structures, can be preserved with paraformaldehyde fixation and Lowicryl embedding.

Immunoreactivity After Paraformaldehyde Fixation

To determine if proteins remain immunoreactive after high-pressure freezing and fixation with paraformaldehyde, we tested previously characterized antibodies for immunoreactivity on ultrathin sections. AF2 is a rabbit polyclonal antibody raised against the *C. elegans* plectin homologue VAB-10A, an epitope that is also recognized by the monoclonal antibody MH5 (Bosher et al. 2003). At the light level, both MH5 and AF2 generate a distinct staining pattern that is limited to periodic foci in the epidermis (Bosher et al. 2003), a pattern reminiscent of fibrous organelle localization in the epidermis. Fibrous organelles attach muscle cells to the underlying cuticle (Hresko et al. 1999; Bercher et al. 2001; Hong et al. 2001; Karabinos et al. 2001). Immunogold labeling demonstrates that VAB-10A is a component of these fibrous organelles. Specifically, at the ultrastructural level AF2 localizes gold particles to fibrous organelles in the epidermis (signal-to-noise >146; see Materials and Methods) (Figure 4).

MH27 is a mouse monoclonal antibody initially raised against worm muscle protein extract (Francis and Waterston 1991) and recognizes the cell adhesion junction protein AJM-1 (Koppen et al. 2001). MH27 has been used previously to label cell junctions with immunogold in larvae after microwave energy fixation (Koppen et al. 2001). Similarly, we observed that MH27 localized gold particles to cell adhesion sites of intestinal cells in adult worms (signal-to-noise >17; see Materials and Methods) (Figure 5). The specificity of immunogold labeling by AF2 and MH27 antibodies demonstrates that proteins remain immunoreactive after high-pressure freezing, fixation with paraformaldehyde, and embedding in Lowicryl.

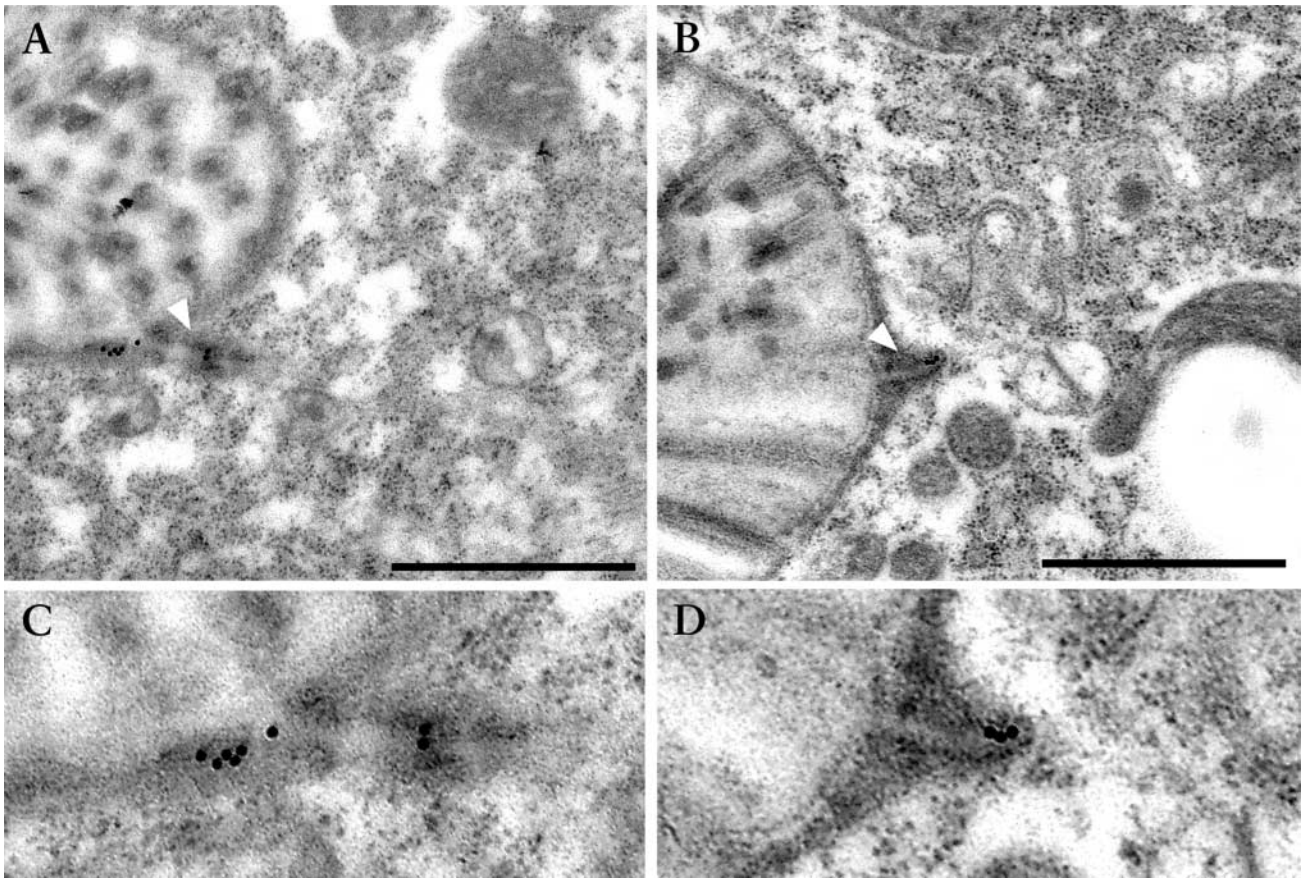

Figure 5 The cell adhesion junction protein AJM-1 remains antigenic after high-pressure freezing. The monoclonal antibody MH27 that recognizes the cell adhesion junction protein AJM-1 localizes gold particles to cell adhesion sites in the intestine (white arrowhead). **(A,B)** Micrographs from two independent staining experiments. Bars = 1000 nm. **(C,D)** Twofold enlargements of **A** and **B**, respectively.

Protein Localization in Neurons

Previous protocols available for immunoelectron microscopy studies in *C. elegans* have been unable to preserve neurons for ultrastructural analysis. However, we observe that neurons are well preserved even in animals embedded in Lowicryl (Figure 3D), suggesting that this protocol may allow the study of protein localization in neurons at the ultrastructural level. To test this assumption, we incubated sections with a monoclonal antibody directed against UNC-17 (Lickteig et al. 2001), the *C. elegans* vesicular acetylcholine transporter (Alfonso et al. 1993). Because UNC-17 is specifically localized to synaptic vesicles in cholinergic neurons, the anti-UNC-17 antibody should localize gold particles to synaptic vesicles in a subset of neurons. Consistent with this notion, we observed that gold particles accumulated in a subset of neurons from sections stained with anti-UNC-17 antibody (Figures 6A and 6B; signal-to-noise ratio >14). In these neurons, the average distance between a gold particle and a synaptic vesicle is 4.7 ± 1.6 nm (n=11) and the distance of the same particles to a microtubule, another abundant structure in presynaptic terminals, is 29.1 ± 8.2 nm (n=11) (Figures 6C and 6D). Therefore, anti-UNC-17 antibodies detect an antigen present on synaptic vesicles, in agreement with the known localization of vesicular acetylcholine transporters. These data demonstrate that protein localization can be studied in neurons at the ultrastructural level after high-pressure freeze immobilization.

Localization of a Protein Tagged with GFP

As mentioned above, engineered proteins, such as protein fusions with the exogenous protein GFP, can be expressed readily in *C. elegans* and used for protein localization studies at the light level. To test whether GFP is a suitable exogenous tag for immunoelectron microscopic studies after our fixation protocol, we stained sections collected from transgenic animal expressing GFP with the polyclonal anti-GFP antibody a11122 (Molecular Probes). The transgene *oxEx81* expresses GFP from the *acr-5* promoter as a chimeric

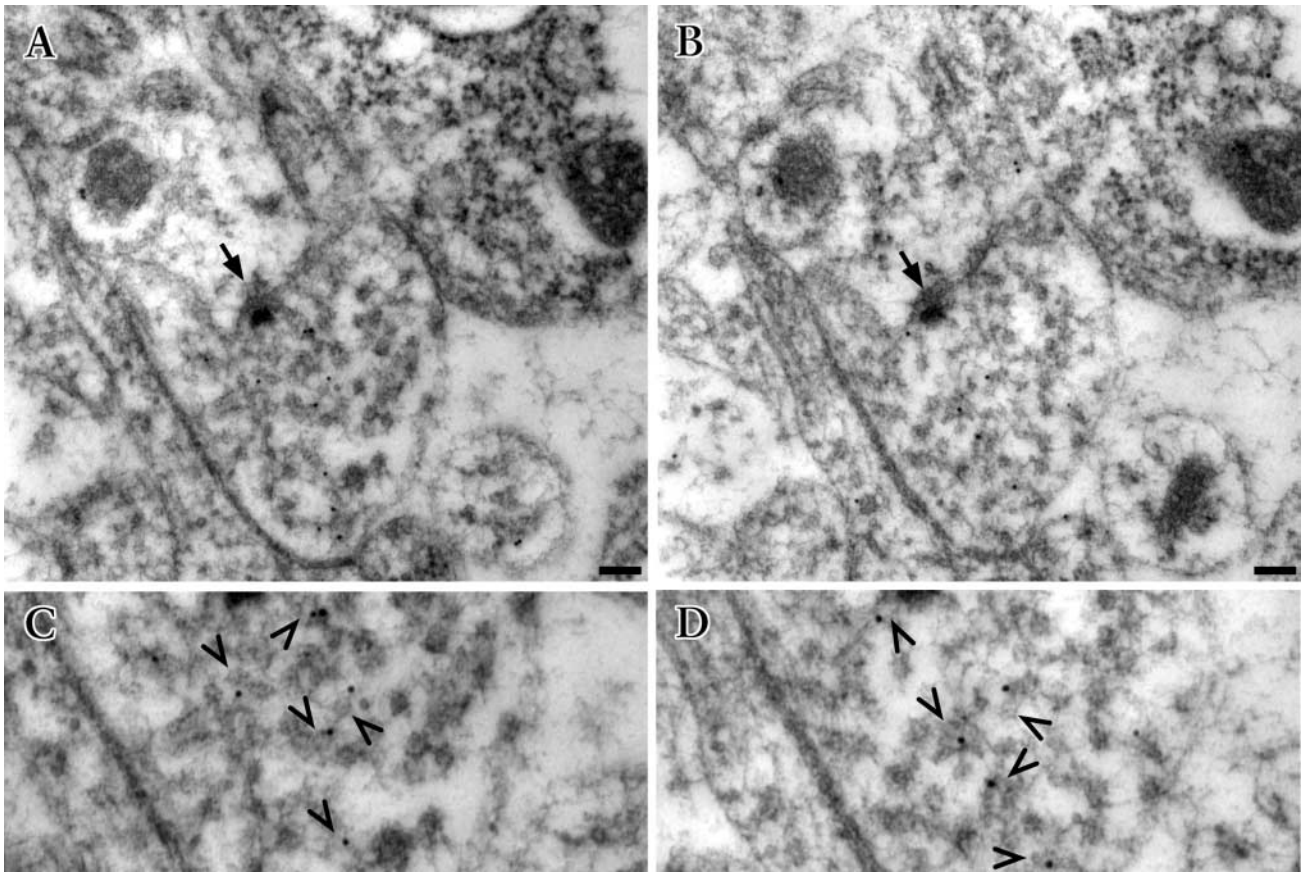

Figure 6 The synaptic vesicle protein UNC-17 remains antigenic after high-pressure freezing. (**A,B**) Serial micrographs of a synaptic profile in the nerve ring stained with the monoclonal anti-UNC-17 antibody. Arrows indicate synapses. Bars = 100 nm. (**C,D**) 1.6-fold enlargements of **A** and **B**, respectively. Open arrowheads indicate synaptic vesicles associated with a 10-nm gold particle.

protein with the myristoylation sequence from GAP-43 (Knobel et al. 2001). In these transgenic worms, GFP is predicted to be localized to membranes in a subset of neuron profiles. After staining with anti-GFP antibodies, gold particles accumulate along the plasma membrane in a subset of neurons in the nerve ring (Figure 7; signal-to-noise ratio >18). These data demonstrate that the exogenous protein tag GFP can be used for ultrastructural localization after high-pressure freeze immobilization.

Discussion

Here we describe a protocol for preserving adult *C. elegans* tissues for morphological and immunological studies at the ultrastructural level. Specifically, living adult animals are immobilized by high-pressure freezing, then chemically fixed in paraformaldehyde and embedded in Lowicryl resin at low temperature. Using this approach, we have been able to characterize the subcellular distribution of proteins in tissues, such as neurons, that were not preserved in previous immunoelectron microscopic studies. This protocol should therefore be suitable for protein localization in most, if not all, *C. elegans* tissues at the ultrastructural level.

Classical Fixation vs High-pressure Freeze Immobilization

Classical ultrastructural analysis of the *C. elegans* anatomy requires the breaching of the animal's cuticle by cutting to allow access of chemical fixatives and embedding resins into the interior tissues. Because the body cavity of *C. elegans* is slightly pressurized, breaching of the animal's cuticle before fixation has the potential to introduce structural artifacts, such as shrinkage of the extracellular space. In addition, the solutions typically used for classical fixation are hyperosmotic, which can exacerbate tissue contraction and membrane ruffling. By contrast, high-pressure freezing arrests tissues in a vitrified state. The vitrified state increases the time window for solutions to penetrate the cuticle and preserve interior tissues.

The importance of this point for morphological studies is illustrated by comparing the morphology of

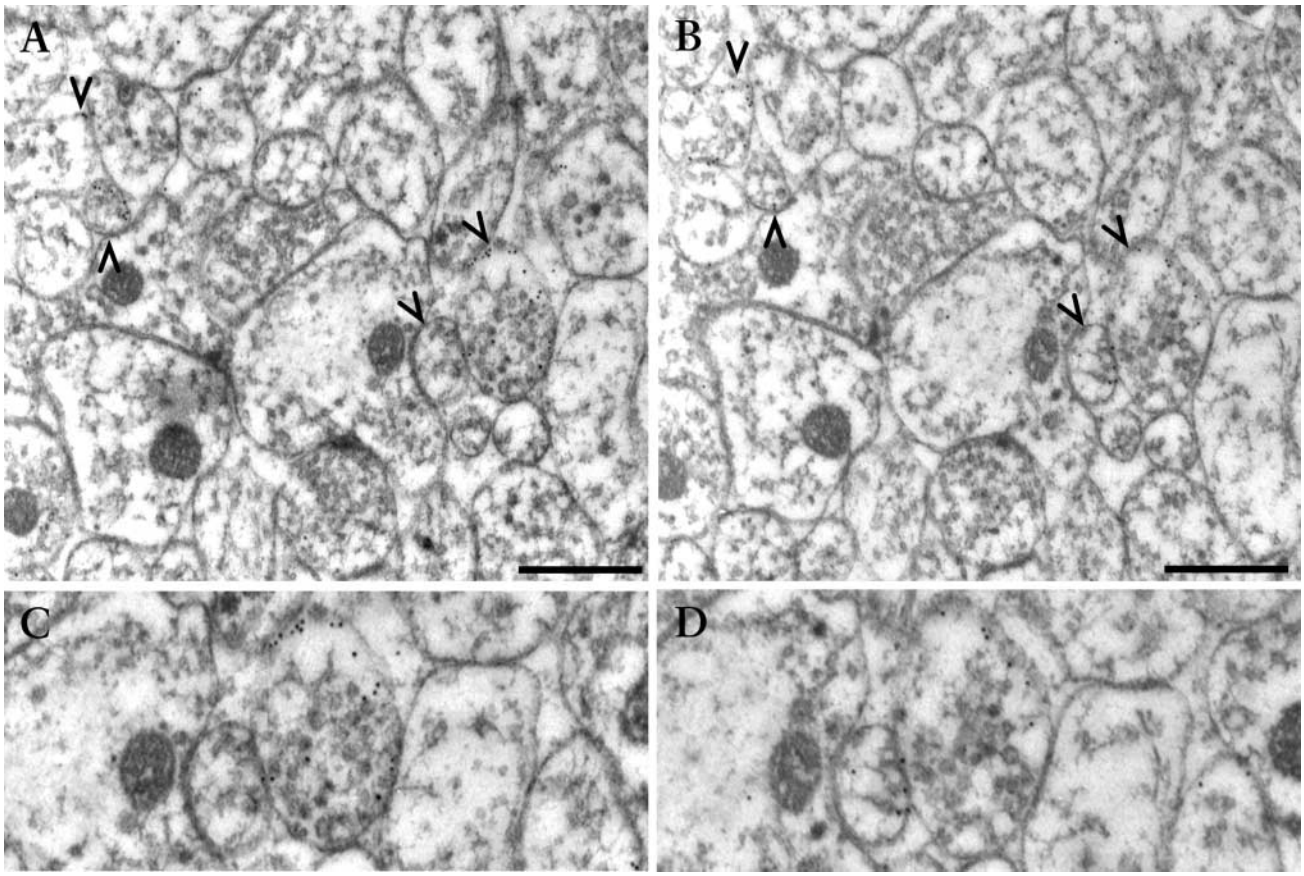

Figure 7 The exogenous protein tag GFP remains antigenic after high-pressure freezing. (**A,B**) Serial micrographs of synaptic profiles stained with the polyclonal anti-GFP antibody 11122 in the nerve ring of a transgenic worm expressing a myristoylated GFP under the control of the *acr-5* promoter. Open arrowheads indicate profiles labeled by 10-nm gold particles. Bars = 100 nm. (**C,D**) 1.5-fold enlargements of **A** and **B**, respectively.

the nerve cord preserved via high-pressure freezing to that which was preserved via classical techniques (Figure 2). After classical techniques, neuron processes are irregularly shaped, with very little space between the processes. However, after high-pressure freezing the neuron processes are round, with regularity in shape and space between processes. It is interesting to note that the average size of membrane structures, such as synaptic vesicles and mitochondria, does not differ between fixation protocols. This suggests that the round appearance of neurons is not due to general swelling of tissues but rather to better preservation of cell morphology by fixation after high-pressure freezing. These observations are consistent with the notion that the morphology observed after high-pressure freezing closely represents the true morphology of tissues in the living animal.

However, membranes appear to be better stained with classical fixation compared to our current fixation protocol. This is probably due to slight differences in the chemistry during fixation at −90C or above freezing. We are now testing whether different concentrations of osmium, various blends of methanol and acetone, or other heavy ions may improve the staining of membranes at very low temperatures.

Morphology of Tissues in Araldite vs Lowicryl

The morphological preservation observed after fixation with osmium tetroxide and embedding in Araldite is outstanding, but both osmium tetroxide and Araldite are incompatible with most immunolabeling. In *C. elegans*, only two cuticle antigens have been labeled thus far using such a protocol (Favre et al. 1995,1998). We failed to observe any staining of osmium-preserved tissues with antibodies that worked using alternative sample processing protocols (PR and RW; data not shown). To circumvent this problem, we substituted paraformaldehyde for osmium tetroxide and Lowicryl for Araldite. At a gross level, the morphology of preserved tissues is similar between the two protocols. For example, overall cell integrity is maintained in all tissues, and intracellular structures,

such as endoplasmic reticulum and mitochondria, are preserved. However, on close inspection differences are observed between the two methods of preservation. Specifically, in the samples processed with paraformaldehyde and Lowicryl, membranes appear slightly fuzzy in all tissues, the organization of the muscle contractile apparatus, particularly the M-line, is not maintained to the same extent, and the continuity of membranous structures is variable compared to the osmium-fixed tissues. These differences are likely due to the fact that Lowicryl HM20 is a soft resin that is difficult to cut and that paraformaldehyde is not as strong a fixative as osmium, especially at these low temperatures. However, at least for the nerve ring, paraformaldehye appears to be dispensable for ultrastructural preservation of high-pressure freeze immobilized tissues. For example, the micrographs shown in Figure 7 are of neuron profiles preserved with methanol fixation alone. Despite the differences between Lowicryl- and Araldite-embedded samples, the level of structural preservation is sufficient for protein localization studies with relation to fine subcellular structures in most tissues, including neurons.

Reproducibility of Morphological Preservation

The usefulness of any technique depends on its reproducibility. We have repeated the paraformaldehyde fixation procedure outlined above a number of times to determine its reproducibility. Thus far, we have observed that the quality of tissue preservation may vary among experiments and even within the same sample. These differences are likely due to small and uncontrolled variability that occurs during the freezing step. Our current solution to this problem involves the freezing and processing of several samples in parallel, followed by the examination of all samples to identify an animal in which the morphology has been well preserved. This animal is then used for subsequent studies. It is interesting to note, however, that every paraformaldehyde-fixed sample tested has retained immunoreactivity, suggesting that whereas morphology may be difficult to preserve, immunoreactivity preservation is robust under these conditions.

Immunolabeling

To date, we have tested and observed immunogold labeling using both monoclonal and polyclonal antibodies generated in mouse and rabbit that recognize antigens present in muscle, epidermis, intestine, and neurons. These successes suggest that this method will be applicable to a number of studies. However, not surprisingly, a few antibodies tested so far (2/7 rabbit antibodies) do not appear to recognize their epitope in sections, which could be due to epitope destruction or masking or due to the staining condition. Therefore, each antibody will need to be tested in an empirical fashion for immunoreactivity on sections. In addition, amplification techniques, such as silver enhancement (Humbel et al. 1995), should be compatible with our fixation/embedding protocol and may aid in the detection of low-abundance proteins. Protein tags, such as GFP, have the potential to alleviate this problem. Once staining conditions are optimized for a particular set of epitope and antibody, these conditions could be used to study the localization of countless tagged proteins.

Application and Potential Uses in Other Systems

The full potential of this technique—cryoimmobilization, weak chemical fixation, and embedding—resides in the fact that proteins are immunolabeled on ultrathin sections after tissue embedding. Therefore, many antibodies and conditions can be tested on sections from the same block of preserved tissue. This eliminates variability in staining due to variation among fixations. In addition, resin-embedded tissues can be maintained over an extended period, making it feasible to accumulate a collection of preserved samples. In the context of a genetic model organism, such as *C. elegans*, one can imagine a library of mutants in embedding blocks. By staining sections from the library, the effects of disrupting a specific protein or pathway on subcellular domains can be characterized at the level of localization of a large number of proteins. Similar tissue libraries could also be constructed of other model organisms, such as *Drosophila*, or of vertebrate tissues, thus accelerating the characterization of protein localization relative to well-preserved subcellular structures in these systems as well.

Acknowledgments

Supported by a grant from the Association Française contre les Myopathies. EMJ and RMW were supported by INSERM Poste Orange and Poste Vert fellowships, respectively.

We thank Kent McDonald and Claude Anthony for kindly sharing many protocols, Jean-Pierre Lechaire and the EM facility of IFR 83 (Paris) for the use of their Bal-Tec HPF, Warren Davis for the micrograph in Figure 2, Michel Labouesse for the anti-VAB-10A antibody, the NICHD for the MH27 antibody, Jim Rand for the anti-UNC-17 antibody, and Marie Delattre for contributing the micrographs presented in Figure 3.

Literature Cited

Albertson DG, Thomson JN (1976) The pharynx of *Caenorhabditis elegans*. Phil Trans R Soc Lond [B] 275:299–325

Alfonso A, Grundahl K, Duerr JS, Han HP, Rand JB (1993) The *Caenorhabditis elegans unc-17* gene: a putative vesicular acetylcholine transporter. Science 261:617–619

Bercher M, Wahl J, Vogel BE, Lu C, Hedgecock EM, Hall DH, Plenefisch JD (2001) *mua-3*, a gene required for mechanical tis-

sue integrity in *Caenorhabditis elegans*, encodes a novel transmembrane protein of epithelial attachment complexes. J Cell Biol 154:415–426

Bosher JM, Hahn BS, Legouis R, Sookhareea S, Weimer RM, Gansmuller A, Chisholm AD, et al. (2003) The *Caenorhabditis elegans vab-10* spectraplakin isoforms protect the epidermis against internal and external forces. J Cell Biol 161:757–768

Brenner S (1974) The genetics of *Caenorhabditis elegans*. Genetics 77:71–94

Chalfie M, Tu Y, Euskirchen G, Ward WW, Prasher DC (1994) Green fluorescent protein as a marker for gene expression. Science 263:802–805

Dernburg AF, McDonald K, Moulder G, Barstead R, Dresser M, Villeneuve AM (1998) Meiotic recombination in *C. elegans* initiates by a conserved mechanism and is dispensable for homologous chromosome synapsis. Cell 94:387–398

Epstein HF, Waterston RH, Brenner S (1974) A mutant affecting the heavy chain of myosin in *Caenorhabditis elegans*. J Mol Biol 90:291–300

Faulk WP, Taylor GM (1971) An immunocolloid method for the electron microscope. Immunochemistry 8:1081–1083

Favre R, Cermola M, Paiva Nunes C, Hermann R, Muller M, Bazzicalupo P (1998) Immuno-cross-reactivity of CUT-1 and cuticlin epitopes between *Ascaris lumbricoides*, *Caenorhabditis elegans*, and *Heterorhabditis*. J Struct Biol 123:1–7

Favre R, Hermann R, Cermola M, Hohenberg H, Muller M, Bazzicalupo P (1995) Immuno-gold-labelling of CUT-1, CUT-2 and cuticlin epitopes in *Caenorhabditis elegans* and *Heterorhabditis sp*. processed by high pressure freezing and freeze-substitution. J Submicrosc Cytol Pathol 27:341–347

Fire A, Waterston RH (1989) Proper expression of myosin genes in transgenic nematodes. EMBO J 8:3419–3428

Fire A, Xu S, Montgomery MK, Kostas SA, Driver SE, Mello CC (1998) Potent and specific genetic interference by double-stranded RNA in *Caenorhabditis elegans*. Nature 391:806–811

Francis R, Waterston RH (1991) Muscle cell attachment in *Caenorhabditis elegans*. J Cell Biol 114:465–479

Hong L, Elbl T, Ward J, Franzini–Armstrong C, Rybicka KK, Gatewood BK, Baillie DL, Bucher EA (2001) MUP-4 is a novel transmembrane protein with functions in epithelial cell adhesion in *Caenorhabditis elegans*. J Cell Biol 154:403–414

Howe M, McDonald KL, Albertson DG, Meyer BJ (2001) HIM-10 is required for kinetochore structure and function on *Caenorhabditis elegans* holocentric chromosomes. J Cell Biol 153:1227–1238

Hresko MC, Schriefer LA, Shrimankar P, Waterston RH (1999) Myotactin, a novel hypodermal protein involved in muscle-cell adhesion in *Caenorhabditis elegans*. J Cell Biol 146:659–672

Humbel BM, Sibon OC, Stierhof YD, Schwarz H (1995) Ultrasmall gold particles and silver enhancement as a detection system in immunolabeling and in situ hybridization experiments. J Histochem Cytochem 43:735–737

Jansen G, Hazendonk E, Thijssen KL, Plasterk RH (1997) Reverse genetics by chemical mutagenesis in *Caenorhabditis elegans*. Nature Genet 17:119–121

Jorgensen EM, Hartwieg E, Schuske K, Nonet ML, Jin Y, Horvitz HR (1995) Defective recycling of synaptic vesicles in synaptotagmin mutants of *Caenorhabditis elegans*. Nature 378:196–199

Karabinos A, Schmidt H, Harborth J, Schnabel R, Weber K (2001) Essential roles for four cytoplasmic intermediate filament proteins in *Caenorhabditis elegans* development. Proc Natl Acad Sci USA 98:7863–7868

Kirkham M, Muller–Reichert T, Oegema K, Grill S, Hyman AA (2003) SAS-4 is a *C. elegans* centriolar protein that controls centrosome size. Cell 112:575–587

Knobel KM, Davis WS, Jorgensen EM, Bastiani MJ (2001) UNC-119 suppresses axon branching in *C. elegans*. Development 128:4079–4092

Koppen M, Simske JS, Sims PA, Firestein BL, Hall DH, Radice AD, Rongo C, et al. (2001) Cooperative regulation of AJM-1 controls junctional integrity in Caenorhabditis elegans epithelia. Nature Cell Biol 3:983–991

Lickteig KM, Duerr JS, Frisby DL, Hall DH, Rand JB, Miller DM III (2001) Regulation of neurotransmitter vesicles by the homeodomain protein UNC-4 and its transcriptional corepressor UNC-37/groucho in *Caenorhabditis elegans* cholinergic motor neurons. J Neurosci 21:2001–2014

MacQueen AJ, Colaiacovo MP, McDonald K, Villeneuve AM (2002) Synapsis-dependent and -independent mechanisms stabilize homolog pairing during meiotic prophase in C. elegans. Genes Dev 16:2428–2442

McDonald K (1999) High-pressure freezing for preservation of high resolution fine structure and antigenicity for immunolabeling. Methods Mol Biol 117:77–97

Mello CC, Kramer JM, Stinchcomb D, Ambros V (1991) Efficient gene transfer in *C. elegans*: extrachromosomal maintenance and integration of transforming sequences. EMBO J 10:3959–3970

Park BJ, Lee DG, Yu JR, Jung SK, Choi K, Lee J, Kim YS, et al. (2001) Calreticulin, a calcium-binding molecular chaperone, is required for stress response and fertility in *Caenorhabditis elegans*. Mol Biol Cell 12:2835–2845

Paupard MC, Miller A, Grant B, Hirsh D, Hall DH (2001) Immuno-EM localization of GFP-tagged yolk proteins in *C. elegans* using microwave fixation. J Histochem Cytochem 49:949–956

Rappleye CA, Paredez AR, Smith CW, McDonald KL, Aroian RV (1999) The coronin-like protein POD-1 is required for anterior-posterior axis formation and cellular architecture in the nematode Caenorhabditis elegans. Genes Dev 13:2838–2851

Rolls MM, Hall DH, Victor M, Stelzer EH, Rapoport TA (2002) Targeting of rough endoplasmic reticulum membrane proteins and ribosomes in invertebrate neurons. Mol Biol Cell 13:1778–1791

Ward S, Thomson N, White JG, Brenner S (1975) Electron microscopical reconstruction of the anterior sensory anatomy of the nematode *Caenorhabditis elegans*. J Comp Neurol 160:313–337

Waterston RH, Epstein HF, Brenner S (1974) Paramyosin of *Caenorhabditis elegans*. J Mol Biol 90:285–290

White JG, Southgate E, Thomson JN, Brenner S (1976) The structure of the ventral nerve cord of *Caenorhabditis elegans*. Phil Trans R Soc Lond [B] 275:327–348

White JG, Southgate E, Thomson JN, Brenner S (1986) The structure of the nervous system of the nematode *Caenorhabditis elegans*. Phil Trans R Soc Lond [B] 314:1–340

Williams–Masson EM, Heid PJ, Lavin CA, Hardin J (1998) The cellular mechanism of epithelial rearrangement during morphogenesis of the *Caenorhabditis elegans* dorsal hypodermis. Dev Biol 204:263–276

Zwaal RR, Broeks A, van Meurs J, Groenen JT, Plasterk RH (1993) Target-selected gene inactivation in *Caenorhabditis elegans* by using a frozen transposon insertion mutant bank. Proc Natl Acad Sci USA 90:7431–7435

The Journal of Histochemistry & Cytochemistry